Engineering Frustrated Lewis Pair Active Sites in Porous Organic Scaffolds for Catalytic CO$_2$ Hydrogenation

Shubhajit Das,[†] Ruben Laplaza,[†,‡] J. Terence Blaskovits,[†] and Clémence Corminboeuf[*,†,‡]

†Laboratory for Computational Molecular Design, Institute of Chemical Sciences and Engineering, École Polytechnique Fedéralé de Lausanne (EPFL), 1015 Lausanne, Switzerland

‡National Center for Competence in Research-Catalysis (NCCR-Catalysis), École Polytechnique Fédérale de Lausanne, 1015 Lausanne, Switzerland

E-mail: clemence.corminboeuf@epfl.ch

1

Summary

Frustrated Lewis pairs (FLPs), featuring reactive combinations of Lewis acids and Lewis bases, have been utilized for myriad homogeneous catalytic processes. Immobilizing the active Lewis sites to a solid support, especially to porous scaffolds, has shown great potential to ameliorate FLP catalysis by circumventing some of its inherent drawbacks, such as product separation and catalyst recyclability. Nevertheless, designing immobilized Lewis pair active sites (LPASs) is challenging due to the requirement of placing the donor and acceptor centers in appropriate geometric arrangements while maintaining the necessary chemical environment to perform catalysis, and clear design rules have not yet been established. In this work, we formulate simple guidelines to build highly active LPASs for direct catalytic hydrogenation of CO_2 through a large-scale screening of a diverse library of 25,000 immobilized FLPs. The library is built by introducing boron-containing acidic sites in the vicinity of the existing basic nitrogen sites of the organic linkers of metal-organic frameworks collected in a "top-down" fashion from an experimental database. The chemical and geometrical appropriateness of these LPASs for CO_2 hydrogenation is determined by evaluating a series of simple descriptors representing the intrinsic strength (acidity and basicity) of the components and their spatial arrangement in the active sites. Analysis of the leading candidates enables the formulation of pragmatic and experimentally-relevant design principles and the leading candidates constitute the starting point for further exploration of FLP-based catalysts for the reduction of CO_2.

1 Introduction

The creation of tailored catalytic active sites to drive a specific chemical transformation is an attractive strategy to design powerful catalysts for sustainable chemical production. The acid-base-nucleophile triad in hydrolase and transferase enzymes,[1] the solid acid pores for hydrocarbon cracking in zeolites,[2] and the nanostructures of electro- and photocatalysts[3] all exemplify local multifunctional environments precisely tailored to minimize the energy requirement of otherwise unlikely transformations. Frustrated Lewis pairs (FLPs), a recent addition to the library of synthetic catalysts, exploit bifunctional environments to drive many catalytic transformations.[4–9] Their unique reactivity is derived from the physical proximity of the Lewis acid (LA) and base (LB) components, in which dative quenching is prevented through constraints of a steric (substituent-based) or geometric (backbone design) nature. Since their inception as molecular catalysts in 2007, the past decade has witnessed tremendous growth in this research area, and the FLP concept has been applied to a broad class of materials including metal/covalent organic frameworks,[10–17] zeolites,[18] mesoporous silica,[19] and metal oxide surfaces.[20–22]
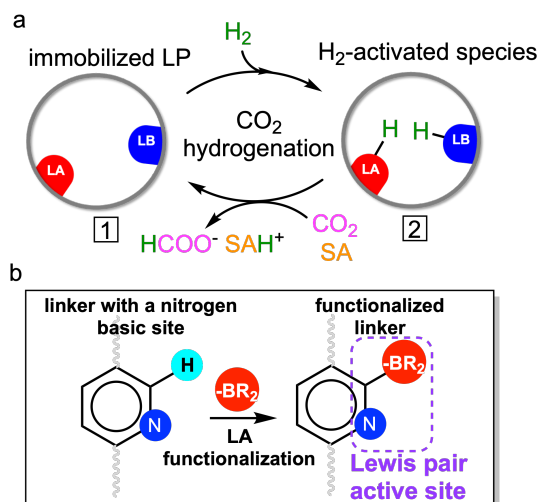
Scheme 1: (a) Simplified description of the immobilized FLP-catalyzed direct hydrogenation of CO_2 to formate. SA represents the sacrificial agent used to drive product release. (b) General strategy to create FLP active sites in porous materials via the functionalization of existing nitrogen-containing organic building blocks.

During the last five years, the incorporation of acid-base components to the rigid backbones of heterogeneous porous scaffolds has emerged as a promising strategy to overcome the inherent drawbacks of molecular FLP catalysts, in terms of stability and recyclability. Several recent reports demonstrated in-situ catalytically active semi-immobilized FLP sites, featuring the combination of one fixed Lewis component embedded in the framework of a host material and another complementary mobile component.[10–14] In most of these studies, the organic building blocks of porous materials, primarily composed of lighter main group elements (H, B, C, N, O, etc.), are a synthetically-relevant starting point for the engineering of such sites. This is due to their structural constituents being similar to those of the most frequently used LAs and LBs in molecular FLP chemistry. Nevertheless, semi-immobilized systems, in principle, could still suffer from recyclability issues owing to one of the catalytic components being soluble. Full immobilization of both the acid and base centers is arguably the most attractive conceptual approach to mitigate this problem. However, this is no trivial task due to the requirement of placing both the acid and base centers in an appropriate geometric position while maintaining the necessary chemical environment of the Lewis pairs to perform a given catalytic reaction of interest.[23,24] The identification of the most promising active site architectures with appropriate chemical and geometrical compositions would thus be invaluable as a starting point for constructing such hybrid active sites. Although the chemical and geometric composition of the FLPs has been individually linked to their performance,[23,24] a clear connection between the full composition of active sites and resulting catalytic performance is currently lacking. Analysis of a broader set of highly active FLP environments will guide the design of catalytic sites and realize the potential of a fully-immobilized catalyst design approach.

Among the various types of porous materials, metal-organic frameworks (MOFs) offer a versatile platform as host materials for FLP sites by virtue of their well-established chemistry and synthetic tunability.[10–17] Here, we exploit an experimental database of MOFs to engineer highly active FLP environments for direct catalytic CO_2 to formate hydrogenation (CTFH),

an important reaction from both an energy and environmental perspective.[25–28] Note that, although stoichiometric FLP-mediated CTFH was first experimentally realized by Ashley *et al.* in 2009,[29] catalytic turnovers were only reported very recently.[23,30] Nitrogen-containing units, particularly pyridine, pyrazoles, imidazoles, triazoles, tetrazoles, and azo moieties, are widespread motifs in the organic linkers of MOFs and they constitute an existing source of chemically and geometrically diverse basic environments to engage in FLP chemistry. These basic nitrogen sites on the organic building blocks of MOFs are utilized to generate all possible FLP environments around them by introducing acidic boron sites in a systematic manner, leading to thousands of potential B/N **L**ewis **p**air **a**ctive **s**ites (LPASs). The chemical and geometrical appropriateness of the generated LPASs are determined and the most promising active site compositions are identified. Analysis of the prospective candidates provides guiding principles for the design of optimal FLP active sites for the reduction of CO_2.
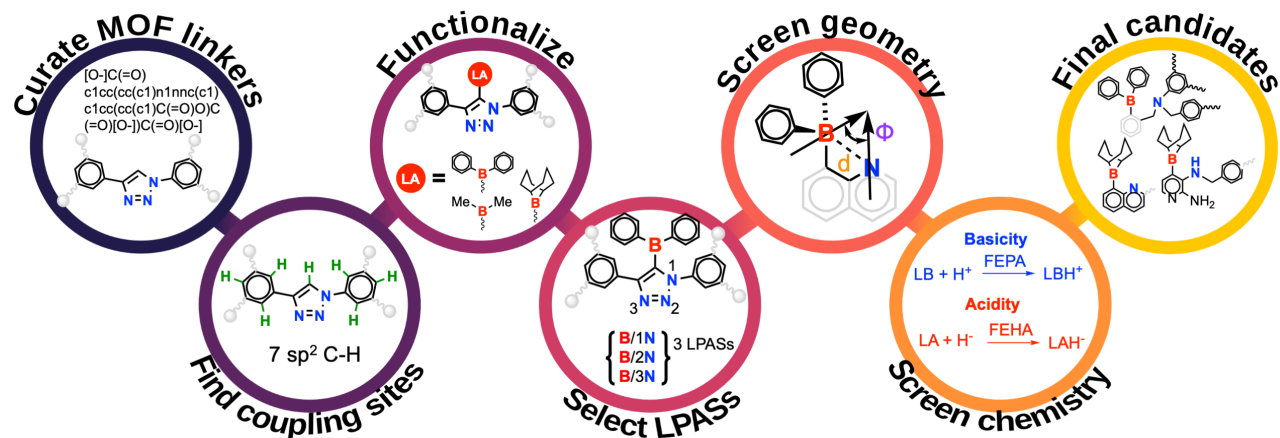

Figure 1: Overview of the workflow for the generation of thousands of LPASs by functionalizing 1043 SLs curated from the CoRE2019 MOF database followed by geometry and chemistry-based screening to identify optimal candidates for CTFH.

2 Results and Discussion

2.1 Library of LPASs

2.1.1 LPAS curation

We selected the CoRE2019 database, which contains a comprehensive collection of synthesized MOFs resulting from many years of experimental work, as the starting point for our study.[31] We begin by top-down curation of 1043 organic linkers (seed linkers or SLs) from this database that have at least one exploitable nitrogen atom as a basic site in an FLP environment (see section S1 for details of the linker curation). After the initial refinement of these linker geometries at a semiempirical level of the theory (GFN2-xTB[32]), a rigorous in-house Python-based protocol was applied, in a bottom-up fashion, to automatically functionalize each of these linkers in all coupling sites with an acidic borane (-BR_2) fragment.[33] The amenable coupling sites are defined as sp^2 carbon atoms with available hydrogens, which were identified using a series of rules based on the connectivity of atoms in each linker geometry. This strategy is motivated by the well-established chemistry of the borylation of arenes, used in the context of FLP chemistry.[34–36] Three -BR_2 units [R= methyl (Me), 9-borabicyclo(3.3.1)nonyl (BBN), phenyl (Ph)] featuring diverse steric and electronic environments were introduced as the LA fragments (Figure 1), which together with the existing nitrogen basic centers constitute the potential FLP sites in the linkers (see Scheme 1b). Each borylation product therefore constitutes a new, albeit synthetically feasible, Lewis-pair-functionalized linker. Since each linker has multiple coupling sites, the functionalization procedure yields 25,522 derivative linkers (DLs). Each DL structure is first optimized at the GFN2-xTB level and then subsequently analyzed to identify the plausible LPAS with the following qualifying criteria: (i) the donor-acceptor distances are within the 2.0-4.0 Å range (ii) the B-O distances are greater than 1.9 Å, and (iii) the N centers are sp^2- or sp^3-hybridized. The distance-based criteria (i) and (ii) eliminate all adduct-forming Lewis pairs due to close proximity between the B and a neighboring N or O (carboxyl) groups, as well as pairs in which the donor

6

and acceptor centers are too far from each other to induce hydrogen activation, which is the first step in the mechanism of the hydrogenation cycle. The second criterion removes all *sp*-hybridized nitrogens (e.g. nitriles/isonitriles) that are presumed to be too weak basic sites for this step. We note that if multiple nitrogen centers are present in the DL structure, the acid unit in principle can satisfy these criteria with more than one nitrogen site, leading to multiple LPAS environments. Overall, 19,720 LPASs were identified to be carried forward to the subsequent screening step.

To illustrate this procedure, we take linker 0010 (corresponding to Core2019 MOF IDs ACAKUM, ACALIB, etc.) as a representative example (Figure 1, first bubble). It has seven $C(sp^2)$-H sites (second bubble); functionalization at each coupling site with -BPh_2 acidic fragments yields seven DLs (and more with the other Lewis acids; third bubble). In each DL, the positioning of the -BPh_2 fragment in the neighborhood of the triazole group leads to the possibility of multiple LPAS depending on which nitrogen serves as the hypothetical Lewis base site. Upon analyzing the optimized geometry of the DLs, only three B-N environments satisfy the criteria of a LPAS (fourth bubble). The rest of the possibilities were discarded due to their non-conformity with the distance criteria or the formation of a quenched boron center (defined by B/O or B/N distances less than 2.0 Å).

2.1.2 Descriptors for the CTFH reactivity of LPASs

The catalytic behavior of an LPAS is determined by its chemical and geometric composition as exemplified by our recent works.[23,24] While the former is associated with the local chemical environment of the Lewis pairs, the latter aspect refers to the spatial arrangements of the donor-acceptor centers in the active site. Thus, the next step is to devise a suitable screening procedure for identifying highly active LPAS considering both the chemistry and geometry of the candidates. Recently, some of us proposed a set of straightforward intuitive chemical and geometrical descriptors which enable a relative comparison of CTFH activity of immobilized B-N FLPs based on minimal active site information (see Figure 2).[23,24]
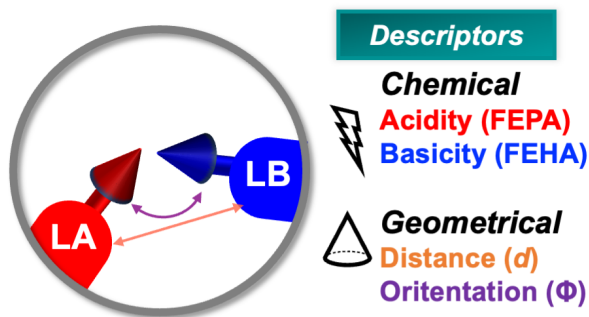
Figure 2: Chemical and geometrical descriptors for CTFH activity of LPASs.

To measure the influence of LPAS geometry on activity, we invoke two descriptors: relative distance (d) and orientation (angle, Φ) of the donor-acceptor units assumed during the catalytic cycle.[24] While d is trivially calculated from the distance between the B and N centers, Φ is estimated from the angle between their open coordination sites for substrate binding. As previously reported by us, the geometric criteria for high CTFH activity stipulate that the LPASs featuring B-N distances between 2.4-3.2 Å **and** relative orientations between 70-140° are substantially more reactive than other geometric arrangements.[24] Note that, it is important to extract the descriptors from the intermediate **2** of the CTFH catalytic cycle to capture the effect of the reaction environment i.e. the inclusion of the H_2 molecule (see Scheme 1a).

Similarly, the effect of chemical composition can be quantified from the individual intrinsic strength of the Lewis components estimated from two descriptors: **f**ree **e**nergy of **h**ydride **a**ttachment (FEHA) and **f**ree **e**nergy of **p**roton **a**ttachment (FEPA) to the corresponding acid and base centers, respectively. Recently, we proposed a computational framework based on linear free energy scaling relationships[37–39] in which these chemical descriptors are mapped to CTFH activity enabling the screening of a database of intermolecular B/N and B/P Lewis pairs.[23] One of the major findings of our study was that the acidity and basicity of the Lewis components need to be appropriately complemented to ensure high catalytic performance. In other words, the cumulative acid-base strength of the pair dictates catalytic activity regardless of the individual strength of the components. Most importantly, the efficacy of

our model was confirmed by the experimental demonstration of the first reported catalytic turnovers in FLP-catalyzed hydrogenation of CO_2.

The four descriptors described above allow the identification of regions of theoretically derived maximum CTFH activity by balancing the acidity and basicity of the Lewis components and by controlling their spatial arrangements.
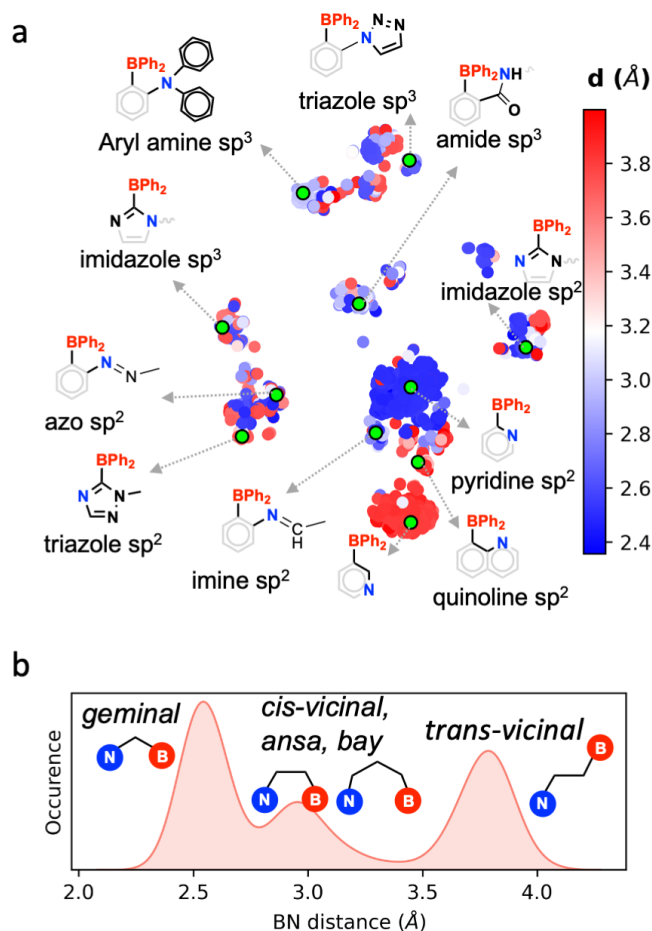

Figure 3: (a) Chemical diversity: 2D t-distributed stochastic neighbor embedding[40] (t-SNE) map of the chemical diversity of all LPASs featuring -BPh_2 as the LA fragment. The embedding was generated from the atomic spectrum of London and Axilrod-Teller-Muto potentials (SLATM) representation of the B and N centers (see section S2 for details). Each point corresponds to an LPAS colored by the B-N distance. Some selected LPASs are shown, which are representative of the various clusters, along with the hybridization and local environment of the nitrogen centers. (b) Geometrical diversity: histogram of the distribution of BN distances in the optimized LPAS geometries.

2.1.3 Diversity of LPASs

The chemical and geometrical diversity of the collection of LPASs with -BPh$_2$ as the acid fragment are illustrated in Figure 3. Figure 3a shows the two-dimensional representation of the chemical diversity using a two-dimensional t-SNE[40] map based on the atomic SLATM[41] representations of the donor (N) and acceptor (B) centers. The vertical axis roughly corresponds to the hybridization of the nitrogen center in the LPAS: sp^3 N sites occupy the upper half of the plot while sp^2 N sites appear at the bottom half (see Figure S8). The horizontal axis captures the variation in nitrogen environments with regard to ring size and number of heteroatoms in the backbone to which it is embedded or attached. The clustering of the different FLP environments is largely based on the distance between the B-N centers as illustrated by some representative systems in Figure 3a. The geometric diversity is shown by the 1D histogram of the B-N distances in the optimized LPAS geometries (Figure 3b). Three major peaks around 2.5 Å 3.0 Å and 3.8 Å in the distance histogram correspond to geminal, *cis*-vicinal/*ansa*/bay, and *trans*-vicinal type spatial arrangements of the Lewis sites, respectively.

2.2 Screening of LPASs

2.2.1 Geometrical criteria

The optimized structures of the curated LPASs are first subjected to a geometry-based screening to recognize the candidates that feature appropriate spatial arrangements in the active sites for the activation of H_2 and subsequent hydride transfer to CO_2.[24] This is primarily due to the stringent nature of the geometric criteria (particularly dominated by Φ) that allow a preliminary screening of the LPAS library and convenient estimation of the relevant descriptors.[24] The geometry of the intermediate **2** for each LPAS was constructed in an automated fashion.[42] The GFN2-xTB-optimized geometries were then filtered to remove fragmented structures, and the geometric descriptors d and Φ were determined.[42] The vast

majority of the LPAS candidates were ruled out by this criterion, leading to a significant reduction of the candidate space. Many of the disqualified LPASs feature geminally-disposed B and N centers (typical d around 2.5 Å); while they satisfy the distance criteria, their relative orientations deem them unsuitable for CTFH, as such closely placed Lewis centers lead to small Φ values. Such orientations are unfavorable for both kinetics of the H_2 activation steps and the thermodynamics of the product release step, both of which have been previously associated with poor CTFH activity.[24] A comparison of the distribution of the Φ values (see Figure S5) reveals that the steric environment of the LA fragment has an impact on determining the orientation, particularly in the prescribed range of high activity; more than 87% of the qualified LPASs contain the larger substituents -BPh_2 and -BBN. The geometries of the candidates satisfying the geometry-based criteria (around 500) were further refined at the PBE0-D3BJ/def2SVP level and the final d and Φ values were collected. These candidates were then carried over for the subsequent chemistry-based screening step.

To estimate the effect of including the linker within the actual MOF structure, a functionalized derivative of the widely used azobenzene-4,4'-dicarboxylic acid (ABDC) linker, termed here 2-BBN-ABDC, was employed to construct a MOF with the primitive cubic (pcu) topology containing a widely-used metal node, Zn_4O (Figure S2). Upon geometry optimization of the MOF at the PBE-D3 level of theory, the geometric descriptors from the linker were extracted (see SI for details). Crucially, these descriptors remain similar to those obtained in the molecular model, implying that the parameters derived from the linkers can be extended to realistic MOF structures.

2.2.2 Chemical criteria

Having identified the LPASs with the appropriate spatial arrangement in the active site, we now search for candidates whose complementary Lewis acidity and basicity are optimal for the reaction in question. The balance between the intrinsic reactivity of the components is visualized in the map presented in Figure 4. Here, by establishing linear free energy
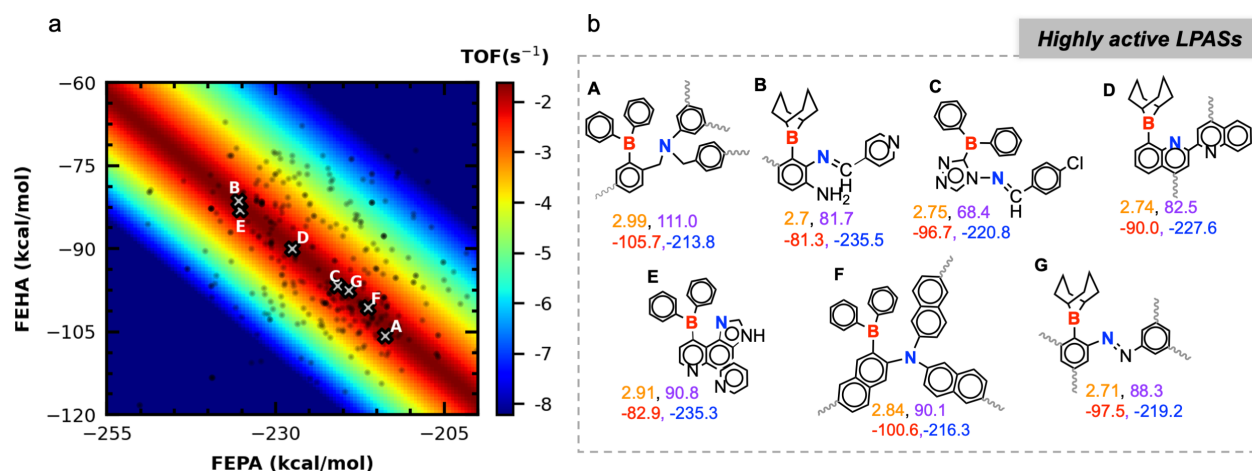
Figure 4: (a) Activity map describing the TOF for the CTFH cycle as a function of FEPA and FEHA for B/N FLPs. Each point represents an LPAS selected from the geometry-based screening step. The TOF is presented in logarithmic scale. (b) The chemical and geometric composition of some prospective LPAS candidates (represented by grey crosses) for CTFH along with four descriptor values (d:orange, Φ:violet, FEHA:red, FEPA:blue). The grey curvy lines indicate carboxyl groups through which the linker is connected to the metal-containing nodes in the MOF structure.

scaling relationships, the theoretically derived TOF for CTFH (plotted along the color axis) is described as a function of FEPA and FEHA (plotted along the x and y axes, respectively). The construction procedure for the activity map is given in the SI (see section S3).[43] The maximum activity region in Figure 4, implying the desired complementarity between acidity and basicity, is indicated by the dark red patch across the map. The LPAS candidates that appear in this region are anticipated to have high CTFH activity since they satisfy both the geometry and chemistry criteria. Upon moving away from the red region to either side, the activity diminishes due to the increasingly difficult product release or higher activation barrier for H_2 cleavage/hydride transfer(Figure S3).[23] The relative CTFH activity of the candidates is compared by placing them on the activity map according to their descriptor values. The sign convention used here defines a more negative FEHA/FEPA value as having a stronger acceptor/donor ability. A broad distribution of FEPA values spanning from -200 to -250 kcal/mol is observed, indicating the diversity of the basic sites present in this subset. Interestingly, for LPASs with a particular LA fragment, the FEHA distribution remains fairly

broad (e.g. -90 to -120 kcal/mol for BPh_2) although comparatively narrower than the FEPA. This implies that the third (aryl) substituent on the boron center, the linker backbone itself, has a strong influence on Lewis acidity of the boron.

Analysis of the composition of the subset of LPASs that satisfy both sets of criteria reveals certain key chemical and geometrical patterns leading to high CTFH activity. By examining some of the representative candidates (Figure 4, right **A**-**G**), it is revealed that stronger LA units (FEHA < -100 kcal/mol) are best paired with weak basic sites such as aryl amines or azo nitrogens, see for example LPAS **A** which features a triaryl borane unit (FEHA=-105.7 kcal/mol) combined with a triaryl amine basic motif (FEPA=-216.2 kcal/mol). Conversely, diminished acidity on the boron sites requires stronger complementary basic sites; in such 'reverse' scenarios, aliphatic, imidazole, and imine basic sites are more appropriate, as in LPAS **B** which features a much weaker BBN-containing LA unit (FEHA=-81.3 kcal/mol) paired to a stronger imine basic unit (FEPA = -235.5 kcal/mol). Finally, LPASs containing LA sites with moderate FEPA values feature basic partners of intermediate strengths (LPAS **C** and **D**). However, a general observation in all of these highly ranked LPASs is that both the B and N centers are somewhat rigidified either by being embedded into a ring system (endocyclic) or by being surrounded by three aryl groups so that the donor and the acceptor centres are locked into a distance and orientation appropriate for CTFH. The most frequently observed compositions involve locking in a *cis*-vicinal arrangement (d and Φ 2.8 Å and 80-90°, respectively), in which the B and N centers are tethered to each other by a two-atom bridge from a six/five-membered aromatic core. Slightly higher separations (2.9 and 3.0 Å in **A** and **E**, respectively) between the Lewis centers are observed in the *ansa* or *bay*-type arrangements, where the nitrogen centers are often part of imidazole or pyrazole cores. The highest angle is observed in **A** (111.0°) due to the *ansa*-type arrangement in which the sp^3 nitrogen takes a benzylic position with respect to the phenyl ring that contains the acid unit. Note that some of these arrangements (vicinal in particular) identified from our screening protocol are structurally similar to intramolecular FLP catalysts which are known

for experimental demonstration of CO_2 hydrogenation.[44]
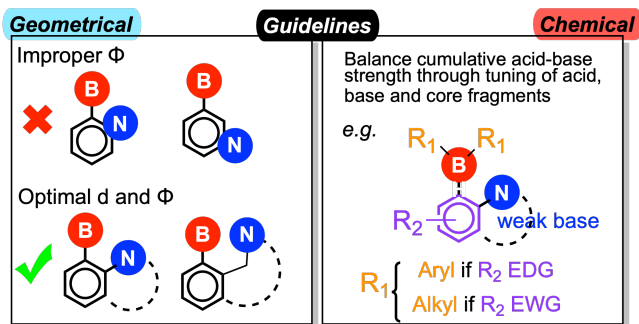
Scheme 2: Geometrical and chemical design rules for constructing highly active LPAS for CTF. EWG/EDG: electron withdrawing/donating groups.

2.3 Guidelines for designing highly active LPASs for CTFH

The above-mentioned analyses lead to the following design principles for the construction of highly active LPASs for CTFH (see Scheme 2). Given a particular basic site that is either embedded within an aromatic core or attached to one, the boron-based acidic site is most effective if it is separated from it by not more than three atoms; otherwise it will hold the donor and acceptor centers at too great a distance (> 4.0 Å) to show any cooperative reactivity (especially for the initial hydrogen activation step). On the other hand, geminal positions should also be avoided as they place the Lewis centers at such short distances that the reaction cavity is not spacious enough (implied by low Φ values) to maintain the proper orientation of the H_2 molecule during bond cleavage. The optimal spatial arrangements are the *cis-vicinal*, *ansa*, and *bay*-type dispositions that offer the appropriate B/N separation and orientation between the acid-base sites required for high catalytic performance. Large acid substituents are generally advisable to maintain the proper orientation between the centers and to avoid quenching with the basic centers. Regarding the chemical composition of the LPAS, the acidity of the boron fragments must be adjusted according to the basicity of the nitrogen site to preserve the cumulative acid-base strength required for high CTFH activity and, unlike the geometry-based requirement, this can be

14

achieved with many different types of acid-base combinations. While choosing the acid fragment, two factors must be considered: (a) the strength of the nitrogen basic site, and (b) the electronic nature of the aromatic core to which it is introduced. For instance, for a weak basic site and an electron-rich core, two aryl substituents on the boron centers provide the complementary Lewis acidity, such as in **F**. This might not be necessary if the core is electron-deficient such as in **G**, where a -BBN unit is sufficiently acidic to complement the weak azo basic site. While we have identified several such chemically balanced LPAS compositions here, many more could be envisioned simply considering the delicate interplay between the factors discussed above. Nevertheless, cumulative strength for any new Lewis pair combination can be readily estimated by computing the corresponding acidity and basicity descriptors using straightforward DFT computations.[23] We note that since these guidelines are derived from a local descriptor-based approach (extracted only from the donor and acceptor fragments), we expect them not to be necessarily limited to MOF linkers but also transferable to a broad family of materials that exploit structurally well-defined organic building blocks such as covalent organic frameworks, porous aromatic frameworks, periodic mesoporous organosilicates, and even polymers. Nevertheless, it should also be pointed out that the present "active site"-based approach does not account for the insertion of CO_2 molecules within the porous channels.

3 Conclusions

In this work, we formulate simple guidelines for designing chemically and geometrically appropriate immobilized Frustrated Lewis Pair active sites that ensure high activity for the direct catalytic hydrogenation of CO_2 to formate. By introducing complementary acidic fragments in the vicinity of intrinsically present nitrogen basic sites present in the organic linkers of MOFs, we construct a sterically and electronically diverse library containing several thousands of possible catalytically active sites. The relative hydrogenation activity

of the candidates in the library is determined by estimating a set of straightforward and intuitive descriptors representing the basicity and acidity of the donor and acceptor centers, respectively, along with their separation distance and orientation relative to one another. This enables the identification of key chemical and geometrical features responsible for high catalytic activity. Based on these results, we propose several design rules. Spatial donor-acceptor arrangements in the *cis-vicinal*, *ansa*, or bay positions maintain the appropriate distance and orientation required for high activity. We expect that different types of acid-base combinations, resulting from the interplay between the electronic nature of the acid fragments, base fragments, and the associated linker cores, will impart on the engineered active site the cumulative acid-base strength desired for high activity. Several such FLP environments are identified and may be incorporated in a broad range of materials (e.g. covalent organic frameworks, coordination polymers, or porous aromatic frameworks). These results lay the groundwork for further exploration of immobilized active sites for important catalytic transformations.

4   Data and code availability

All data will be made available as a Materials Cloud repository. The *crosscoupler* tool used to functionalize the linkers in the seed database is available on GitHub at `https://github.com/lcmd-epfl/FORMED_ML`

5   Acknowledgements

References

(1) Dodson, G.; Wlodawer, A. Catalytic triads and their relatives. *Trends in biochemical sciences* **1998**, *23*, 347–352.

(2) Bhatia, S. *Zeolite catalysts: principles and applications*; CRC press, 1989.

(3) Liu, M.; Pang, Y.; Zhang, B.; De Luna, P.; Voznyy, O.; Xu, J.; Zheng, X.; Dinh, C. T.; Fan, F.; Cao, C., et al. Enhanced electrocatalytic CO 2 reduction via field-induced reagent concentration. *Nature* **2016**, *537*, 382–386.

(4) Erker, G.; Stephan, D. W. *Frustrated Lewis Pairs*; Springer, 2013; Vol. 1.

(5) Stephan, D. W.; Erker, G. Frustrated Lewis pairs: metal-free hydrogen activation and more. *Angewandte Chemie International Edition* **2010**, *49*, 46–76.

(6) Stephan, D. W.; Erker, G. Frustrated Lewis pair chemistry: development and perspectives. *Angewandte Chemie International Edition* **2015**, *54*, 6400–6441.

(7) Erker, G.; Stephan, D. W. *Frustrated Lewis pairs II: expanding the scope*; Springer, 2013; Vol. 334.

(8) Stephan, D. W. Frustrated lewis pairs. *Journal of the American Chemical Society* **2015**, *137*, 10018–10032.

(9) Stephan, D. W. The broadening reach of frustrated Lewis pair chemistry. *Science* **2016**, *354*.

(10) Niu, Z.; Gunatilleke, W. D. B.; Sun, Q.; Lan, P. C.; Perman, J.; Ma, J.-G.; Cheng, Y.; Aguila, B.; Ma, S. Metal-organic framework anchored with a Lewis pair as a new paradigm for catalysis. *Chem* **2018**, *4*, 2587–2599.

(11) Shyshkanov, S.; Nguyen, T. N.; Chidambaram, A.; Stylianou, K. C.; Dyson, P. J. Frustrated Lewis pair-mediated fixation of CO 2 within a metal–organic framework. *Chemical Communications* **2019**, *55*, 10964–10967.

(12) Shyshkanov, S.; Nguyen, T. N.; Ebrahim, F. M.; Stylianou, K. C.; Dyson, P. J. In Situ Formation of Frustrated Lewis Pairs in a Water-Tolerant Metal-Organic Framework for the Transformation of CO2. *Angewandte Chemie International Edition* **2019**, *58*, 5371–5375.

(13) Meng, Q.; Huang, Y.; Deng, D.; Yang, Y.; Sha, H.; Zou, X.; Faller, R.; Yuan, Y.; Zhu, G. Porous Aromatic Framework Nanosheets Anchored with Lewis Pairs for Efficient and Recyclable Heterogeneous Catalysis. *Advanced Science* **2020**, *7*, 2000067.

(14) Zhang, Y.; Lan, P. C.; Martin, K.; Ma, S. Porous frustrated Lewis pair catalysts: Advances and perspective. *Chem Catalysis* **2022**,

(15) Liu, Q.; Liao, Q.; Hu, J.; Xi, K.; Wu, Y.-T.; Hu, X. Covalent Organic Frameworks Anchored with Frustrated Lewis Pairs for Hydrogenation of Alkynes with H2. *Journal of Materials Chemistry A* **2022**,

(16) Ye, J.; Johnson, J. K. Screening Lewis pair moieties for catalytic hydrogenation of CO2 in functionalized UiO-66. *ACS Catalysis* **2015**, *5*, 6219–6229.

(17) Ye, J.; Johnson, J. K. Design of Lewis pair-functionalized metal organic frameworks for CO2 hydrogenation. *ACS Catalysis* **2015**, *5*, 2921–2928.

(18) Lee, H.; Choi, Y. N.; Lim, D.-W.; Rahman, M. M.; Kim, Y.-I.; Cho, I. H.; Kang, H. W.; Seo, J.-H.; Jeon, C.; Yoon, K. B. Formation of Frustrated Lewis Pairs in Ptx-Loaded Zeolite NaY. *Angewandte Chemie* **2015**, *127*, 13272–13276.

(19) Zakharova, M. V.; Masoumifard, N.; Hu, Y.; Han, J.; Kleitz, F.; Fontaine, F.-G.

Designed Synthesis of Mesoporous Solid-Supported Lewis Acid–Base Pairs and Their CO2 Adsorption Behaviors. *ACS applied materials & interfaces* **2018**, *10*, 13199–13210.

(20) Wang, L.; Kehr, G.; Daniliuc, C. G.; Brinkkötter, M.; Wiegand, T.; Wübker, A.-L.; Eckert, H.; Liu, L.; Brandenburg, J. G.; Grimme, S., et al. Solid state frustrated Lewis pair chemistry. *Chemical science* **2018**, *9*, 4859–4865.

(21) Dong, Y.; Ghuman, K. K.; Popescu, R.; Duchesne, P. N.; Zhou, W.; Loh, J. Y.; Jelle, A. A.; Jia, J.; Wang, D.; Mu, X., et al. Tailoring Surface Frustrated Lewis Pairs of In2O3- x (OH) y for Gas-Phase Heterogeneous Photocatalytic Reduction of CO2 by Isomorphous Substitution of In3+ with Bi3+. *Advanced Science* **2018**, *5*, 1700732.

(22) Zhang, S.; Huang, Z.-Q.; Ma, Y.; Gao, W.; Li, J.; Cao, F.; Li, L.; Chang, C.-R.; Qu, Y. Solid frustrated-Lewis-pair catalysts constructed by regulations on surface defects of porous nanorods of CeO 2. *Nature communications* **2017**, *8*, 1–11.

(23) Das, S.; Turnell-Ritson, R. C.; Dyson, P. J.; Corminboeuf, C. Design of Frustrated Lewis Pair Catalysts for Direct Hydrogenation of CO2. *Angewandte Chemie International Edition* **2022**,

(24) Das, S.; Laplaza, R.; Blaskovits, J. T.; Corminboeuf, C. Mapping Active Site Geometry to Activity in Immobilized Frustrated Lewis Pair Catalysts. *Angewandte Chemie* **2022**, e202202727.

(25) Wang, W.-H.; Himeda, Y.; Muckerman, J. T.; Manbeck, G. F.; Fujita, E. CO2 hydrogenation to formate and methanol as an alternative to photo-and electrochemical CO2 reduction. *Chemical reviews* **2015**, *115*, 12936–12973.

(26) Alvarez, A.; Bansode, A.; Urakawa, A.; Bavykina, A. V.; Wezendonk, T. A.; Makkee, M.; Gascon, J.; Kapteijn, F. Challenges in the greener production of formates/formic acid, methanol, and DME by heterogeneously catalyzed CO2 hydrogenation processes. *Chemical reviews* **2017**, *117*, 9804–9838.

(27) Klankermayer, J.; Wesselbaum, S.; Beydoun, K.; Leitner, W. Selective catalytic synthesis using the combination of carbon dioxide and hydrogen: catalytic chess at the interface of energy and chemistry. *Angewandte Chemie International Edition* **2016**, *55*, 7296–7343.

(28) Liu, Q.; Wu, L.; Jackstell, R.; Beller, M. Using carbon dioxide as a building block in organic synthesis. *Nature communications* **2015**, *6*, 5933.

(29) Ashley, A. E.; Thompson, A. L.; O'Hare, D. Non-metal-mediated homogeneous hydrogenation of CO2 to CH3OH. *Angewandte Chemie International Edition* **2009**, *48*, 9839–9843.

(30) Wang, T.; Xu, M.; Jupp, A. R.; Qu, Z.-W.; Grimme, S.; Stephan, D. W. Selective catalytic frustrated Lewis pair hydrogenation of CO2 in the presence of silylhalides. *Angewandte Chemie* **2021**, *133*, 25975–25979.

(31) Chung, Y. G.; Haldoupis, E.; Bucior, B. J.; Haranczyk, M.; Lee, S.; Zhang, H.; Vogiatzis, K. D.; Milisavljevic, M.; Ling, S.; Camp, J. S., et al. Advances, updates, and analytics for the computation-ready, experimental metal–organic framework database: CoRE MOF 2019. *Journal of Chemical & Engineering Data* **2019**, *64*, 5985–5998.

(32) Bannwarth, C.; Ehlert, S.; Grimme, S. GFN2-xTB—An accurate and broadly parametrized self-consistent tight-binding quantum chemical method with multipole electrostatics and density-dependent dispersion contributions. *Journal of chemical theory and computation* **2019**, *15*, 1652–1671.

(33) Blaskovits, J. T.; Laplaza, R.; Vela, S.; Corminboeuf, C. Data-driven discovery of organic electronic materials enabled by hybrid top-down/bottom-up design. *ChemRxiv* **2022**, DOI: 10.26434/chemrxiv–2022–88t32.

(34) Mkhalid, I. A.; Barnard, J. H.; Marder, T. B.; Murphy, J. M.; Hartwig, J. F. C- H activation for the construction of C- B bonds. *Chemical Reviews* **2010**, *110*, 890–931.

(35) Heiden, Z. M.; Schedler, M.; Stephan, D. W. Synthesis and reactivity of o-benzylphosphino-and o-α-methylbenzyl (N, N-dimethyl) amine-boranes. *Inorganic chemistry* **2011**, *50*, 1470–1479.

(36) Légaré, M.-A.; Courtemanche, M.-A.; Rochette, É.; Fontaine, F.-G. Metal-free catalytic CH bond activation and borylation of heteroarenes. *Science* **2015**, *349*, 513–516.

(37) Greeley, J. Theoretical heterogeneous catalysis: scaling relationships and computational catalyst design. *Annual review of chemical and biomolecular engineering* **2016**, *7*, 605–635.

(38) Calle-Vallejo, F.; Loffreda, D.; Koper, M. T.; Sautet, P. Introducing structural sensitivity into adsorption–energy scaling relations by means of coordination numbers. *Nature chemistry* **2015**, *7*, 403–410.

(39) Busch, M.; Wodrich, M. D.; Corminboeuf, C. Linear scaling relationships and volcano plots in homogeneous catalysis–revisiting the Suzuki reaction. *Chemical science* **2015**, *6*, 6754–6761.

(40) Van der Maaten, L.; Hinton, G. Visualizing data using t-SNE. *Journal of machine learning research* **2008**, *9*.

(41) Huang, B.; von Lilienfeld, O. A. Quantum machine learning using atom-in-molecule-based fragments selected on the fly. *Nature Chemistry* **2020**, *12*, 945–951.

(42) During construction of intermediate **2**, LPASs containing trans-vicinally disposed BN centers were not considered as it would yield improper geometry of the intermediate.

(43) Laplaza, R.; Das, S.; Wodrich, M. D.; Corminboeuf, C. Constructing and interpreting volcano plots and activity maps to navigate homogeneous catalyst landscapes. *Nature Protocols* **2022**, 1–20.

(44) Courtemanche, M.-A.; Pulis, A. P.; Rochette, É.; Légaré, M.-A.; Stephan, D. W.; Fontaine, F.-G. Intramolecular B/N frustrated Lewis pairs and the hydrogenation of carbon dioxide. *Chemical Communications* **2015**, *51*, 9797–9800.